

# Chapter 19

## Fossil Methane Seep Deposits and Communities from the Mesozoic of Antarctica



James D. Witts and Crispin T. S. Little

### 19.1 Introduction

Fossil methane seep deposits are rare in the Mesozoic of the Southern Hemisphere and especially in the high palaeolatitudes of Antarctica. This rarity is also reflected in the relatively small number of present-day methane seep and hydrothermal vent communities known from around the continent, which is the subject of ongoing research (e.g. Römer et al. 2014; Bell et al. 2016; Linse et al. 2019). Perhaps unsurprisingly, given the relatively small area of the continent that is ice-free and permits geological study, only two occurrences of fossil methane seep deposits have been reported from Antarctica (Fig. 19.1). Both are located on islands surrounding the Antarctic Peninsula region, which because of the lack of significant vegetation at this latitude offers exceptional outcrop conditions. These seep deposits are related to the accumulation of thick sedimentary sequences deposited in forearc and back-arc settings during the Jurassic (Tithonian) and Cretaceous (Maastrichtian), adjacent to a long-lived active magmatic arc.

### 19.2 Alexander Island

The fossil methane seep from the uppermost Jurassic (Tithonian) Fossil Bluff Group exposed on Alexander Island (AI) (Fig. 19.1b), Antarctica, is of interest given its remoteness from other Jurassic seep faunas. The seep locality was initially described

---

J. D. Witts (✉)

School of Earth Sciences, University of Bristol, Bristol, UK

e-mail: [james.witts@bristol.ac.uk](mailto:james.witts@bristol.ac.uk)

C. T. S. Little

School of Earth & Environment, University of Leeds, Leeds, UK

e-mail: [earctsl@leeds.ac.uk](mailto:earctsl@leeds.ac.uk)

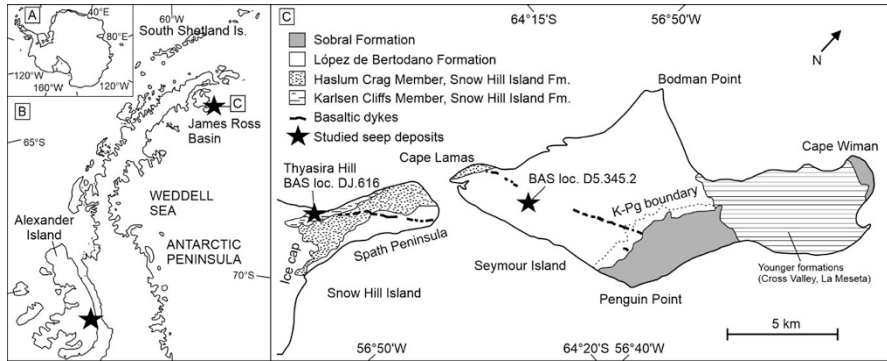


**Fig. 19.1** Locality map of Antarctica (a) and Antarctic Peninsula Region (b), showing general location of fossiliferous methane seep deposits (black stars) on Alexander Island and the James Ross Basin. (position of (c) indicated). (c) Outline geological map of Seymour Island and the NE tip of Snow Hill Island, James Ross Basin. (Modified from Crame et al. (2004), Little et al. (2015), and Tosolini et al. (2021))

by Kelly et al. (1995) who provided lithological and preliminary faunal descriptions, as well as taphonomic and geochemical data. The seep carbonates form a laterally discontinuous limestone body known as the Gateway Pass Limestone Bed (GPLB). A description of hokkaidoconchid gastropods, the dominant faunal element at the seep, was provided by Kaim and Kelly (2009). Beyond these two papers, this locality is unstudied, and we provide only a brief overview here.

### 19.2.1 Location and Geological Setting of AI

The >7000-m-thick Fossil Bluff Group outcrops across the eastern coast of AI, bounded to the east by the present George VI Ice Shelf and to the west by the accretionary complex Le May Group, which it is faulted against and unconformably overlies. It represents the clastic fill of a forearc basin succession to the west of the active magmatic arc of the Antarctic Peninsula during the late Jurassic and early Cretaceous (Doubleday et al. 1993). Rifting in the Kimmeridgian formed a deep-marine basin, filled initially by hemipelagic muds, overlain in places by a large-scale (tens of km) slope mass-transport complex and succeeded by deep-marine channel-levee complexes (Butterworth and Macdonald 2007).

The Fossil Bluff Group is divided into five formations (Doubleday et al. 1993). The ~1.1-km-thick Atoll Nunatacks Formation (ANF) occurs towards the base of the group and comprises thinly bedded mudstones and silty mudstones representing a marine transgression followed by deposition of turbidites in a trench-slope setting. It probably indicates a phase of subsidence in response to contemporaneous tectonic events in the adjacent accretionary prism (Doubleday et al. 1993). This area may have been located at 60–70°S during the Tithonian (Lawver et al. 1992), but

complex terrane tectonics in this region place some doubt as to the palaeolatitude of AI prior to the mid-Cretaceous (Vaughan and Storey 2000).

### ***19.2.2 Age of ANF***

The precise age of the seep locality within the ANF is not well constrained. Faunal data from radiolaria (Holdsworth and Nell 1992) and a sparse molluscan fauna containing buchiid bivalves and belemnopsid belemnites constrain deposition to the Bathonian–Tithonian (Doubleday et al. 1993). The seep carbonates occur towards the upper part of the succession and are, therefore, considered Tithonian in age.

### ***19.2.3 Brief Description of Seep Localities on ALI***

The GPLB is exposed discontinuously for around 200 m between scree-filled gullies on Offset Ridge, AI (68°39'W, 71°38'S), ~2 km east of the LeMay Range Fault Zone, which represents the boundary between forearc and accretionary prism deposits (Kelly et al. 1995). It varies from 3 m at its thickest at the east end of the outcrop where the base is not exposed, pinching out westwards. The seep carbonates themselves are composed of calcite-cemented mudstones and sandstones covered by irregular laminated crusts up to 2-m wide and 20-cm thick, which are in places brecciated (Kelly et al. 1995; Kaim and Kelly 2009). Mass aggregations of fossils occur in mudstone interbeds associated with the crusts. Four phases of calcite and silica cement formed within the crusts. The cemented crusts exhibit depleted  $\delta^{13}\text{C}$  values of  $-40.8\%$  to  $-44.6\%$ , while sparry cement infills range from  $-33.5\%$  to  $-40.5\%$ , both typical of the anaerobic oxidation of methane (AOM).

Kelly et al. (1995) interpreted the seep as potentially forming on a palaeobathymetric high, but within a pockmark structure on the seafloor with carbonate crusts forming around the mouth of the seep. The source of the methane is unclear, but up to 2 km of the Fossil Bluff Group underlies the horizon containing the seep. Kelly et al. (1995) speculated that structural features and faulting focused methane migration within the basin, and identified a nearby synsedimentary normal fault as a conduit, with brecciation evidence for occasional gas ponding and explosions.

### ***19.2.4 Fauna of the GPLB***

The GPLB is characterized by increased faunal abundance compared to the rest of the relatively unfossiliferous ANF. The seep fauna is dominated by high-spined gastropods, originally described as 'cerithiforms' by Kelly et al. (1995). Kaim and Kelly (2009) redescribed these as a new species of seep obligate hokkaidoconchid,

*Hokkaidoconcha hignalli*. These gastropods are associated with large lucinids, protobranch bivalves, as well as rare limpets, crinoids, belemnites and ammonites (Kelly et al. 1995; Kaim and Kelly 2009). Microfossils (ostracods and foraminifera) are also present. *Thalassinoides* burrows and *Trypanites* borings occur in the limestone crusts (Kelly et al. 1995). Abundant gastropod faecal pellets were documented by Kaim and Kelly (2009). Dark-clotted laminae and blebs within the crusts themselves may represent fossilized *Beggiatoa*-type bacterial mats.

The faunal association of hokkaidoconchids and lucinids in the AI seep is very reminiscent of Jurassic and Cretaceous fossil seep communities from Japan (Kaim et al. 2008) and the US Pacific Coast (Kiel et al. 2008), suggesting that a widespread seep fauna was present around the margins of the Pacific during this part of the Mesozoic.

### 19.3 James Ross Basin

Methane seeps from uppermost Cretaceous (Maastrichtian) volcanoclastic shallow shelf sediments exposed on Snow Hill and Seymour Islands, James Ross Basin (JRB) (Fig. 19.1b), Antarctica were documented in detail by Little et al. (2015). The seeps are manifest as large, cement-rich carbonate bodies on Snow Hill Island and micrite-cemented burrow systems on Seymour Island (Fig. 19.1c). They are associated with a low diversity fauna of thyasirid, solemyid and lucinid bivalves.

#### 19.3.1 Location and Geological Setting of the JRB

The JRB is a large extensional sedimentary basin that formed behind the magmatic arc of the Antarctic Peninsula from the late Mesozoic to early Cenozoic (e.g. Pirrie et al. 1997; Crame et al. 2004; Olivero 2012). The volcanoclastic sediments deposited in this basin are now exposed on various islands in the James Ross Island area, including Snow Hill and Seymour Islands (subsequently SHI and SI, respectively; Fig. 19.1), and represent the best onshore sedimentary sequence of its age in the southern high latitudes. Because of its importance and fossiliferous nature, this region has been the focus of a large number of studies (see Crame 2019 for a recent review).

The Late Cretaceous-Paleogene infill of the JRB comprises >2500 m of fine-grained sediments, part of which forms the Coniacian to Danian aged Marambio Group (Pirrie et al. 1997; Crame et al. 2004; Olivero 2012; Milanese et al. 2020). The middle-upper part of the Group comprises most of the Snow Hill Island Formation (SHIF) and overlying López de Bertodano (LBF) and Sobral (SF) formations (Fig. 19.2). Tectonic reconstructions and magnetostratigraphic data suggest that the JRB was located at ~65°S during the Late Cretaceous-Paleogene (Lawver et al. 1992; Milanese et al. 2019a).

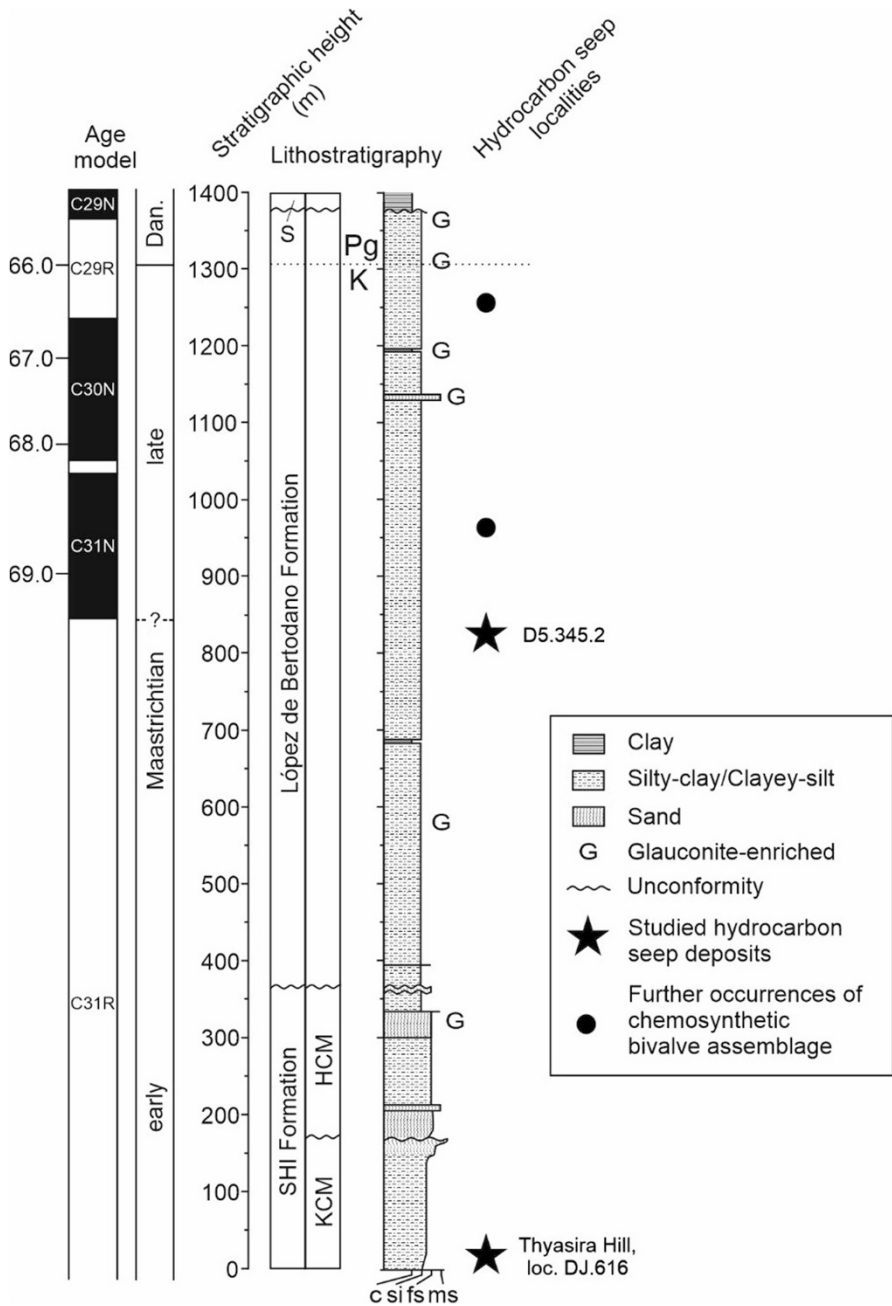


**Fig. 19.2** Composite stratigraphy of the Maastrichtian part of the Marambio Group on Snow Hill and Seymour Islands, following Pirrie et al. (1997), Crame et al. (2004) and Bowman et al. (2013) for lithostratigraphy and biostratigraphy, and Tobin et al. (2012), Bowman et al. (2013), Montes et al. (2019) and Milanese et al. (2019b) for age model. Stars mark the approximate positions of the studied hydrocarbon seep deposits. Black circles indicate other occurrences of chemosynthetic bivalve assemblage ('*Thyasira*'; '*Lucina*'; '*Solemya*') collected during British Antarctic Survey (BAS) expeditions in 1999 and 2006 (see Witts et al. (2016) for details). Abbreviations: *SHI* Snow Hill Island, *KCM* Karlsen Cliffs Member, *HCM* Haslum Crag Member, *S* Sobral Formation, *K* Cretaceous, *Pg* Paleogene, *Dan* Danian

The top two units of the SHIF on SHI are the Karlsen Cliffs Member (KCM) below and the Haslum Crag Member (HCM) above (Fig. 19.2). These two units crop out on the Spath Peninsula at the northern tip of SHI, and along strike on the southwestern tip of SI. The KCM consists of mudstones, sandy mudstones and heavily bioturbated fine sandstones with abundant early diagenetic concretions (Pirrie et al. 1997), interpreted by Olivero (2012) as representing sediments formed in a coarsening upwards prograding deltaic wedge. The HCM of Pirrie et al. (1997) is roughly equivalent to the Haslum Crag Sandstone of Olivero (2012) and comprises medium- to coarse-grained cross-stratified and channelized sandstones, passing upwards into intensely bioturbated fine-grained sandstones and siltstones, containing fossiliferous concretions (Pirrie et al. 1997). The HCM is separated from the KCM and overlying LBF by unconformities (Pirrie et al. 1997; Crame et al. 2004). Olivero (2012) interpreted the Haslum Crag Sandstone as being forced regressive tidal deposits (Olivero 2012; fig. 2). The LBF crops out on the eastern side of the Spath Peninsula of SHI (lower part only) and extensively on the western side of SI (full thickness; Fig. 19.2). The LBF contains the Cretaceous-Paleogene (K-Pg) boundary and mass extinction event near its top (Fig. 19.2; Zinsmeister 1998; Crame et al. 2004; Witts et al. 2016). Lithologically, the LBF is dominated by intensely bioturbated muddy siltstones, with thin intercalated sandstones and discontinuous concretionary levels. The LBF coarsens upwards slightly towards the top of the section where there are some prominent glauconitic sandstones (Crame et al. 2004). According to Olivero (2007), the lower part of the LBF comprises estuarine and shallow marine deposits, the middle part transgressive shelf deposits and the top part regressive shelf deposits (Olivero 2012; fig. 2). The LBF is overlain by the Sobral Formation (SF), which out crops on the eastern and northern sides of SI and records deposition in a range of prodelta and shallow deltaic environments (Marensi et al. 2012; Bowman et al. 2016; Whittle et al. 2019).

### 19.3.2 Age of the JRB Sequence

Ammonites provide the best biostratigraphic zonation of the JRB Cretaceous sequence (Macellari 1986; Olivero 2012; Witts et al. 2015). Olivero and Medina (2000) and Olivero (2012) divided the Cretaceous succession into 14 ammonite assemblages, based mainly on the stratigraphic distribution of the family Kossmaticeratidae. The KCM and HCM occur in assemblage 10, while the overlying LBF contains assemblages 11 to 14. Ammonite taxa from the KCM, HCM and LBF are all indicative of a Maastrichtian age (Macellari 1986; Olivero 2012; Witts et al. 2015). This is in agreement with microfossil data from dinoflagellate cysts (Bowman et al. 2012). Palynological data also support assignment of the upper part of the LBF above the K-Pg boundary and most of the overlying Sobral Formation on SI to the Danian (Elliot et al. 1994; Bowman et al. 2016).

Magnetostratigraphic study of the JRB Cretaceous and early Paleogene sequence has recently been completed (Fig. 19.2). These data suggest the KCM on SHI

correlates in its entirety to magnetochron C31R (Milanese et al. 2019b). The LBF on SI spans chrons C31R through C29N and was, therefore, deposited between ~70 and 65.7 Ma (Tobin et al. 2012). The overlying SF contains chrons C29N to C26R and was deposited between 65.7 and ~62 Ma (Montes et al. 2019).

### 19.3.3 Description of Fossil Seep Localities in the JRB

#### 19.3.3.1 Carbonate Bodies and ‘Thyasira’ Occurrences on Snow Hill Island

As reported in Little et al. (2015), specimens of the large thyasirid bivalve ‘*Thyasira townsendi*’ are common in the lower part of the type section of the KCM on the Spath Peninsula, SHI, especially at the locality known as ‘*Thyasira Hill*’ (British Antarctic Survey (BAS) locality DJ.616) (64.37°48’S, 56.98°07’W) (Pirrie et al. 1997) (Figs. 19.3, 19.4, and 19.5g). In places at this locality, thyasirid fossils reach an estimated density of >120/m<sup>2</sup> (Fig. 19.3c). Clusters of ‘*T. townsendi*’ are associated with patches of pale blue-grey carbonate cementation which serve to accentuate the regular, planar bedding (Fig. 19.3b, d). At the bottom of the section, the cemented regions are 20 to 30 cm thick and 50 to 100 cm in width, but at higher levels in the succession, the beds are more continuous and weather out to form the peak of a prominent structure 60 m in height that forms the summit of *Thyasira Hill* (Figs. 19.3a and 19.4a, c). This feature is located approximately 500 m SW of ‘Nordenskjöld’s Hut’, a historic structure erected as a winter station by the Swedish South Polar Expedition in the early twentieth century (see Zinsmeister 1988; Almevik et al. 2021).

At *Thyasira Hill*, carbonate-cemented, sheet-like shell beds are 30 to 75 cm thick (Figs. 19.3e and 19.4c). Many ‘*T. townsendi*’ shells are in growth position but rarely touch each other (Figs. 19.4c and 19.5a); others are clearly *ex situ* and broken. Small specimens of ammonites (*Gunnarites antarcticus* and indeterminate lycoceratids) are also preserved in the cemented layers (Fig. 19.3e). Interbeds have yielded isolated specimens of ‘*T. townsendi*’ together with ammonites, including *Jacobites anderssoni* (Fig. 19.5f), *Gunnarites bhavaniformis* (Fig. 19.5e) and scattered specimens of the serpulid worm *Austrorotularia* sp. About 200 m across a small valley to the South of *Thyasira Hill* at the same stratigraphic level are approximately 12 topographic knolls up to 10 m tall and ~5 m wide (Fig. 19.4b, d), which represent carbonate-cemented patches that have been exhumed by weathering from the enclosing fine-grained sediments. These knolls have similar lithologies and faunal content to *Thyasira Hill*, including the ammonite *Gunnarites antarcticus*, the solemyid bivalve *Solemya rossiana* and indeterminate gastropods. Well-cemented ‘*Thyasira*’ patches and carbonate layers are discontinuous both laterally and vertically within the KCM, occurring through an approximately 50-m-thick section, and over 100 m horizontally.

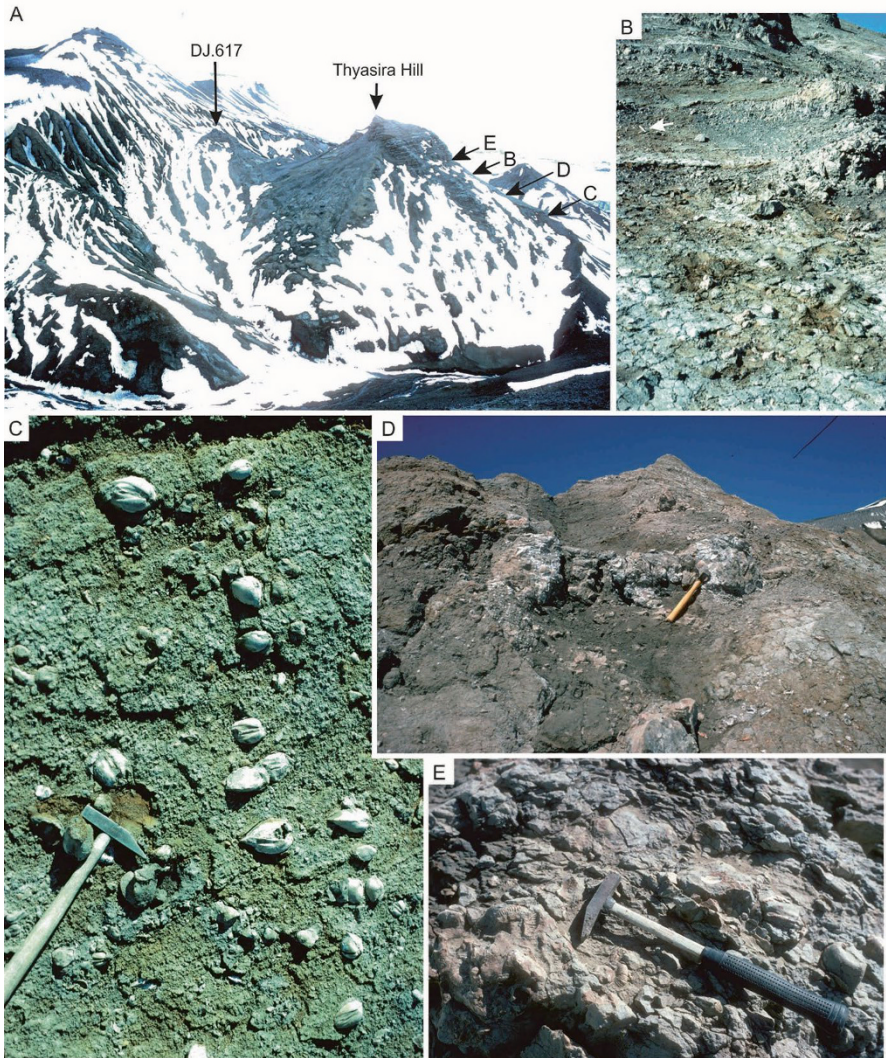


**Fig. 19.3** Field images of carbonate-cemented sediments and associated fossils from the Karlsen Cliffs Member, near Nordenskjolds Hut, Snow Hill Island, looking toward the SW. Section (a) runs from the base of the hill, bottom right of the photograph, up the slope through points where photographs (c–e) were taken, over Thyasira Hill. Cliffs at the top left of photograph a are the Haslum Crag Member. The white arrow points in the younging direction, perpendicular to dip of the beds. (b) and (d) Irregularly shaped patches of carbonate-cemented sediments. (c) *In-situ* articulated ‘*Thyasira townsendi*’ specimens in plain view on the surface of an exposed bedding plane. (e) Ammonites and articulated ‘*Thyasira townsendi*’ specimens, base of Thyasira Hill. Geological hammers are for scale in (b) (see white arrow), (c), (d) and (e) approximately 40 cm long

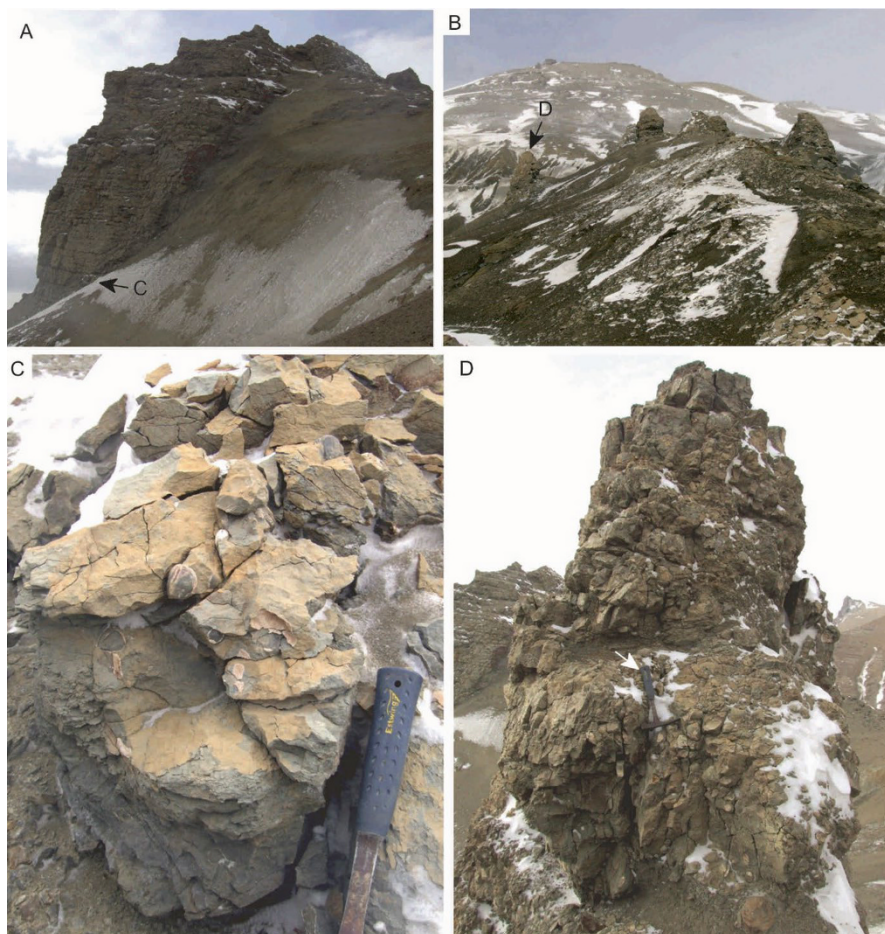


**Fig. 19.4** Field images of carbonate-cemented sediments and associated fossils from Karlens Cliffs Member, Snow Hill Island. (a) Thyasira Hill; arrows show position of image (c). (b) Knolls of exhumed carbonate-cemented sediment, approximately 200 m East of Thyasira Hill; arrow shows position of photo (d). Outcrops in the hills in background are Haslum Crag Member. (c) Detail of (a) showing carbonate-cemented sediment enclosing weathered articulated ‘*Thyasira*’ *townsendi* specimens. (d) Detail of knoll in (b) with Thyasira Hill in background, to left; arrow points to hammer scale. Geological hammers are for scale in (c) and (d) approximately 30 cm long

Little et al. (2015) interpreted the laterally discontinuous carbonate-cemented sediments at the *Thyasira* Hill locality on SHI as representing methane seeps formed during a period of increasingly concentrated hydrocarbon seepage. Cement phases from the SHI carbonates and infill within articulated ‘*T.*’ *townsendi* fossils exhibit  $\delta^{13}\text{C}$  values between -20.4‰ and -10.7‰. Molecular fossils extracted from the seep carbonates are indicative of micro-organisms involved in AOM such as methanotrophic archaea and suggest dominance of thermogenic methane over other hydrocarbons (Little et al. 2015).

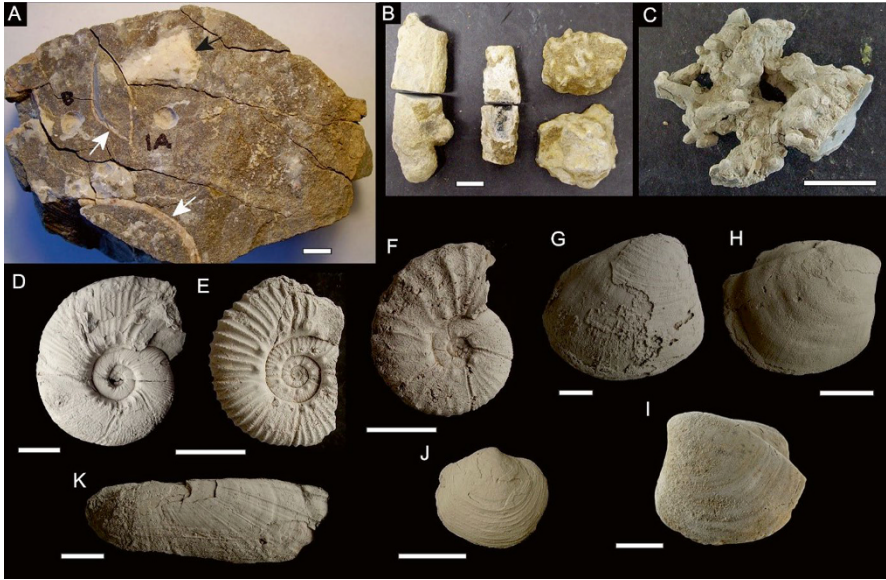


**Fig. 19.5** Fossils and carbonate concretions from methane seep deposits on Snow Hill and Seymour Islands, Antarctica. **(a)** Hand specimen of carbonate-cemented siltstone from Thyasira Hill, Karlens Cliffs Member, Snow Hill Island. White arrows point to articulated '*Thyasira townsendi*' specimens in various sections. Black arrow points to sparry calcite cement patch. Codes 1A and B are sites drilled for isotopic analysis in Little et al. (2015). **(b)** Cut tubular carbonate concretion from BAS locality D5.345.2, López de Bertodano Formation, Seymour Island. Note the presence of small *Planolites*-like burrows on the surface of the concretion. **(c)** Carbonate concretion of cemented large burrows with smaller burrows on their surfaces; from Hydrate Hole seep site, 3100 m water depth, Congo deep-sea fan (Haas et al. 2010). **(d)** Ammonite *Maorites seymourianus* from BAS locality D5.347.2, López de Bertodano Formation, Seymour Island. **(e)** Ammonite *Gunnarites* sp. (possibly *G. bhavaniformis*) from Thyasira Hill, Snow Hill Island. **(f)** Ammonite *Jacobites anderssoni* from BAS locality DJ.633.1, Thyasira Hill, Karlens Cliffs Member, Snow Hill Island. **(g)** Right valve of articulated '*Thyasira townsendi*' from Thyasira Hill, Snow Hill Island. **(h)** Right valve of articulated specimen of bivalve '*Thyasira townsendi*' from BAS locality D5.345.2, López de Bertodano Formation, Seymour Island; internal mould. **(i)** Left valve of articulated large thyasirid bivalve from Deception Island, Antarctica (specimen 1464 from PRI, New York). **(j)** Right valve of articulated specimen of bivalve '*Lucina scotti*' from BAS locality D5.345.2, López de Bertodano Formation, Seymour Island. **(k)** Right valve of bivalve *Solemya rossiana*, BAS locality D5.345.2, López de Bertodano Formation, Seymour Island. All fossils are whitened with ammonium chloride powder. Scale bars **a–c** = 10 mm; **d–k** = 20 mm

### 19.3.3.2 Carbonate Concretions and '*Thyasira*' Occurrences on Seymour Island

'*Thyasira townsendi*' itself occurs intermittently in laterally discontinuous layers, usually within a distinctive dark sulphurous mudstone facies, throughout the rest of the nearly 1500-m-thick Maastrichtian succession on SHI and SI (Fig. 19.2), often in association with articulated specimens of the lucinid '*Lucina scotti*' (Fig. 19.5j) and/or the solemyid *Solemya rossiana* (Fig. 19.5k). Stratigraphically, later '*T*'

*townsendi* layers in the HCM and LBF are, however, not associated with well-cemented large carbonate deposits like those in the KCM.

Little et al. (2015) studied one of these horizons from the LBF of SI (BAS locality D5.345.2), ~458 m above the basal unconformity with the HCM (Fig. 19.2). This locality contains scattered cylindrical and carbonate-cemented concretions up to 39 mm in length composed of dark fine-grained sediments cemented by micrite with a later, weathering rind of gypsum (Fig. 19.5b). Some concretions have internal infillings of fibrous calcite cements. Others are roughly circular and have pale-coloured *Planolites*-like burrows on their surfaces, strongly resembling modern seep-associated concretions (Fig. 19.5c) (Haas et al. 2010). Associated with these are abundant specimens of '*T.* *townsendi*' (Fig. 19.5h), *S. rossiana* (Fig. 19.5k) and some examples of the ammonites *Maorites seymourianus* (Fig. 19.5d) and *M. weddelliensis*. Benthic molluscs are also associated with this concretionary layer, such as the nuculid and trioniid bivalves *Leionucula suboblunga* and *Oistotrigonia pygoscelium*, and the gastropod '*Cassidaria*' mirabilis. These are typical of the 'background' benthic molluscan fauna found throughout the LBF on SI (Zinsmeister and Macellari 1988; Crame et al. 2014; Witts et al. 2016). The last occurrence of the distinctive '*T.* *townsendi*' facies is a prolifically fossiliferous bedding plane ~48 m below the K-Pg boundary in the upper levels of the LBF (Fig. 19.2) (Witts et al. 2016).

Little et al. (2015) concluded that the laterally discontinuous concretionary layers with putatively chemosymbiotic bivalves present throughout the LBF on SI were methane seeps that formed during repeated periods of diffuse methane flux to the sediment. Depleted carbon isotope values within concretionary matrix and cements range from -58.0‰ to -24.6‰ and suggest AOM together with an increased contribution of biogenic methane compared to the older SHI seeps. Geochemical data (specifically depleted  $\delta^{13}\text{C}$  values) derived from shell material of well-preserved bivalves and ammonites at discrete intervals throughout the LBF also suggest that these periodic intervals of increased methane flux may have influenced the chemistry of the sediments, overlying water column and organisms inhabiting these environments (Tobin and Ward 2015; Hall et al. 2018; Ivany and Artruc 2020).

### 19.3.4 Fauna of the JRB Methane Seeps

The JRB methane seep fauna is dominated by the large thyasirid bivalve '*T.* *townsendi*', often co-occurring together with the lucinid bivalve '*Lucina*' *scotti* and/or the solemyid bivalve *Solemya rossiana* (Zinsmeister and Macellari 1988; Crame et al. 2014; Witts et al. 2016). Little et al. (2015) suggested that these taxa very likely had symbionts like many living representatives of these families, and that association of these species with the seep carbonates in the KCM and LBF indicated the presence of AOM-derived hydrogen sulphide. Other studies have found petrological and geochemical evidence for fluctuating redox conditions in these sections, possibly on a seasonal scale (Schoepfer et al. 2017). However, the presence of a

diverse ‘background’ benthic molluscan fauna, both epi- and infauna, associated with the chemosymbiotic taxa in the KCM and LBF indicates that environmental conditions in the sediment were not persistently challenging.

Interestingly, the JRB methane seep fauna does not include representatives of other common Mesozoic and Cenozoic seep obligate taxa, such as *Paskentana*, hokkaidoconchids, *Peregrinella*, *Caspiconcha*, vesicomids or bathymodiolins. The reasons for this are unclear, but may be related to the high palaeolatitude of the JRB, the relatively shallow (<200 m) water depths in the basin, palaeoecology, or simply that the Maastrichtian age of the succession is earlier than the evolution of some of these taxa (see discussion in Little et al. 2015).

*Thyasira townsendi* specimens from SHI were first described by Weller (1903) and identified as being conspecific with White’s (1890) species *Lucina townsendi* from Cretaceous sediments on St. Paul’s and St. Peter’s Islands in the Magellan Strait. Wilckens (1910) later suggested that *Lucina townsendi* (White) 1890 is not a lucinid and transferred the species to the genus *Thyasira*. However, as noted by Zinsmeister and Macellari (1988), ‘*Thyasira townsendi* is much larger than other *Thyasira* species, and in size and shape more resembles species belonging to *Conchocele* (Kamenev et al. 2001; Okutani, 2002; Oliver and Sellanes, 2005), hence the placement of the genus name ‘*Thyasira*’ in quotation marks here and in Little et al. (2015). Large thyasirid bivalves with very similar morphologies to ‘*T. townsendi*’ are also found in other Cretaceous deposits in the high Southern latitudes, including specimens from Deception Island, Antarctica (Fig. 19.5i) and the species *T. bullpointensis* (Stilwell) from North Island, New Zealand.

Similarly, the shell morphology of ‘*Lucina scotti*’ (Wilckens) (Fig. 19.5j) 1910 does not correspond well to this genus (or to Wilckens’ original genus *Phacoides*). The Antarctic species very likely belongs to the extinct lucinid genus *Nymphalucina* Speden, 1970 (Kiel 2013), which is particularly well known from seep and non-seep environments in the Cretaceous Western Interior Seaway in North America (Kauffman et al. 1996; Ryan et al. 2020), because of the external characters, and the shape of the cardinal teeth that can be seen in some weathered articulated JRB specimens.

It seems unlikely that any of the three bivalve taxa common at JRB seep localities were seep obligates. Both ‘*L. scotti*’ (commonly) and *S. rossiana* (rarely) occur throughout the LBF, apparently not always in association with seep carbonates (Zinsmeister and Macellari, 1988). A single specimen of ‘*T. townsendi*’ was also recently documented from the 237- to 250-m level in the Palaeocene SF, i.e., ~315 m above the K-Pg boundary. The upper levels of the SF have also yielded several small specimens of a solemyid that appears to represent a new species (Crame et al. 2014; Whittle et al. 2019). Other lucinid bivalves (previously assigned to *Saxolucina*) occur sporadically throughout the LBF and SF (Stilwell et al. 2004; Beu 2009; Crame et al. 2014; Whittle et al. 2019). The precise taxonomic placement of these bivalves, and whether their occurrence coincides with additional periods of hydrocarbon seepage in the JRB, remains to be elucidated.

**Acknowledgements** We thank Alistair Crame, Jane Francis, Rowan Whittle and Vanessa Bowman (British Antarctic Survey) for assistance and useful discussions about the JRB and Antarctic palaeontology. Thanks also to the co-authors of the Little et al. (2015) study (Daniel Birgel, Adrian Boyce, Steffen Kiel, Jörn Peckmann, Duncan Pirrie and Gavyn Rollinson). Hilary Blagborough is thanked for providing access to BAS specimens and collections. We are grateful to Neil Landman (AMNH) and Kirk Cochran (Stony Brook University) for their encouragement and opportunity to write this contribution and helpful reviews.

## References

- Almevik G, Avango D, Contissa V et al (2021) Built cultural heritage in Antarctica. Remains and uses of the first Swedish South Polar expedition 1901–1903. Report from the Expert and Research Expedition CHAQ2020, Swedish National Heritage Board, p 169
- Bell JB, Aquilina A, Woulds C et al (2016) Geochemistry, faunal composition and trophic structure in reducing sediments on the southwest South Georgia margin. *Roy Soc Open Sci* 3:160284
- Beu AG (2009) Before the ice: biogeography of Antarctic Paleogene molluscan faunas. *Palaeogeogr Palaeoclim Palaeoecol* 284:191–226
- Bowman VC, Francis JE, Riding JB et al (2012) A latest Cretaceous to earliest Paleogene dinoflagellate cyst zonation from Antarctica, and implications for phytoprovincialism in the high southern latitudes. *Rev Palaeobot Palynol* 171:40–56
- Bowman VC, Francis, JE, Riding, JB (2013) Late Cretaceous winter sea ice in Antarctica? *Geology* 41:1227–1230
- Bowman V, Ineson J, Riding J et al (2016) The Paleocene of Antarctica: Dinoflagellate cyst biostratigraphy, chronostratigraphy and implications for the palaeo-Pacific margin of Gondwana. *Gondwana Res* 38:132–148
- Butterworth P, Macdonald D (2007) Channel-levee complexes of the Fossils Bluff Group, Antarctica. In: Nilson T, Shew R, Steffens G, Studlick J (eds) AAPG Atlas of deepwater outcrops. American Association of Petroleum Geologists Special Publication, Tulsa, pp 36–41
- Crame JA (2019) Paleobiological significance of the James Ross Basin. *Adv Polar Sci* 30:186–198
- Crame JA, Francis JE, Cantrill DJ, Pirrie D (2004) Maastrichtian stratigraphy of Antarctica. *Creta Res* 25:411–423
- Crame JA, Beu AG, Ineson JR et al (2014) The Early Origin of the Antarctic Marine Fauna and Its Evolutionary Implications. *PLoS One* 9:e114743
- Doubleday PA, Macdonald DIM, Nell PAR (1993) Sedimentology and structure of the trench-slope to forearc basin transition in the Mesozoic of Alexander Island, Antarctica. *Geol Mag* 130:737–754
- Elliot DH, Askin RA, Kyte FT, Zinsmeister WJ (1994) Iridium and dinocysts at the Cretaceous-Tertiary boundary on Seymour Island, Antarctica: implications for the K-T event. *Geology* 22:675–678
- Haas A, Peckmann J, Elvert M et al (2010) Patterns of carbonate authigenesis at the Kouilou pockmarks on the Congo deep-sea fan. *Mar Geol* 268:129–136
- Hall JLO, Newton RJ, Wits JD et al (2018) High benthic methane flux in low sulfate oceans: Evidence from carbon isotopes in Late Cretaceous Antarctic bivalves. *Earth Planet Sci Lett* 497:113–122
- Holdsworth BK, Nell PR (1992) Mesozoic radiolarian faunas from the Antarctic Peninsula: age, tectonic and palaeoceanographic significance. *J Geol Soc (London)* 149:1003–1020
- Ivany LC, Artruc EG (2020) Lifespan, growth rate, and ecology of a giant heteromorph ammonite from Antarctica. Paper presented at the Annual Meeting of the Geological Society of America, GSA Connects Online, 25–28 October 2020

- Kaim A, Kelly SRA (2009) Mass occurrence of hokkaidoconchid gastropods in the Upper Jurassic methane seep carbonate from Alexander Island, Antarctica. *Antarct Sci* 21:279–284
- Kaim A, Jenkins RG, Warén A (2008) Provannid and provannid-like gastropods from the Late Cretaceous cold seeps of Hokkaido (Japan) and the fossil record of the Provannidae (Gastropoda: Aabysochrysoidea). *Zool J Linne Soc* 154:421–436
- Kamenev GM, Nadochy VA, Kuznetsov AP (2001) *Conchocele bisecta* (Conrad, 1849) (Bivalvia: Thyasiridae) from cold-water methane-rich areas of the Sea of Okhotsk. *Veliger* 44:84–94
- Kauffman EG, Arthur MA, Howe B, Scholle PA (1996) Widespread venting of methane-rich fluids in Late Cretaceous (Campanian) submarine springs (Tepee Buttes), Western Interior seaway, U.S.A. *Geology* 24:799–802
- Kelly SRA, Ditchfield PW, Doubleday PA, Marshall JD (1995) An Upper Jurassic methane-seep limestone from the Fossil Bluff Group forearc basin of Alexander Island, Antarctica. *J Sed Res* 65:274–282
- Kiel S (2013) Lucinid bivalves from ancient methane seeps. *J Molluscan Stud* 79:346–363
- Kiel S, Campbell KA, Elder WP, Little CTS (2008) Jurassic and cretaceous gastropods from hydrocarbon seeps in forearc basin and accretionary prism settings, California. *Acta Palaeontol Polonica* 53:679–703
- Lawver LA, Gahagan LM, Coffin MF (1992) The development of Paleoseaways around Antarctica. In: Kennet JP, Warnke DA (eds) *The Antarctic paleoenvironment: a perspective on global change: part one*, vol 56. American Geophysical Union (AGU), Washington, DC, pp 7–30
- Linse K, Copley JT, Connelly DP et al (2019) Fauna of the Kemp Caldera and its upper bathyal hydrothermal vents (South Sandwich Arc, Antarctica). *Roy Soc Open Sci* 6:91501
- Little CTS, Birgel D, Boyce AJ et al (2015) Late Cretaceous (Maastrichtian) shallow water hydrocarbon seeps from Snow Hill and Seymour Islands, James Ross Basin, Antarctica. *Palaeogeog Palaeoclim Palaeoecol* 418:213–228
- Macellari CE (1986) Late Campanian–Maastrichtian Ammonite Fauna from Seymour Island (Antarctic Peninsula). *J Paleontol* 60:1–55
- Marensi S, Santillana S, Bauer M (2012) Stratigraphy, sedimentary petrology and provenance of the Sobral and Cross Valley formations (Paleocene), Marambio (Seymour) Island, Antarctica. *Andean Geol* 39:67–91
- Milanese F, Rapalini A, Slotznick SP, Tobin TS (2019a) Late Cretaceous paleogeography of the Antarctic Peninsula: new paleomagnetic pole from the James Ross Basin. *J South Am Earth Sci* 91:131–143
- Milanese FN, Olivero EB, Raffi ME et al (2019b) Mid Campanian–Lower Maastrichtian magnetostratigraphy of the James Ross Basin, Antarctica: chronostratigraphical implications. *Basin Res* 31:562–583
- Milanese FN, Olivero EB, Slotznick SP, Tobin TS, Raffi ME, Skinner, SM, Kirschvink, JL, Rapalini AE (2020) Coniacian–Campanian magnetostratigraphy of the Marambio Group: The Santonian–Campanian boundary in the Antarctic Peninsula and the complete Upper Cretaceous–Lowermost Paleogene chronostratigraphical framework for the James Ross Basin. *Palaeogeog Palaeoclim Palaeoecol* 555:109871
- Montes M, Beamud E, Nozal F, Santillana S (2019) Late Maastrichtian–Paleocene chronostratigraphy from Seymour Island, James Ross Basin, Antarctic Peninsula: eustatic controls on sedimentation. *Adv Polar Sci* 61:303–327
- Okutani T (2002) A new thyasirid *Conchocele novaeguineensis* n. sp. from a thanatocoenosis associated with a possible cold seep activity off New Guinea. *Venus (J Malacol Soc Jpn)* 61:141–145
- Oliver PG, Sellanes J (2005) New species of Thyasiridae from a methane seepage area off Concepción, Chile. *Zootaxa* 1092:1–20
- Olivero EB (2012) Sedimentary cycles, ammonite diversity and palaeoenvironmental changes in the Upper Cretaceous Marambio Group, Antarctica. *Cretaceous Res* 34:348–366
- Olivero EB, Medina FA (2000) Patterns of Late Cretaceous ammonite biogeography in southern high latitudes: the family Kossmaticeratidae in Antarctica. *Cretaceous Res* 21:269–279

- Olivero EB, Ponce JJ, Marsicano CA, Martinioni DR (2007) Depositional Settings of the basal López de Bertodano Formation, Maastrichtian, Antarctica. *Revista de la Asociación Geológica Argentina* 62:521–529
- Pirrie D, Crame JA, Lomas SA, Riding JB (1997) Late Cretaceous stratigraphy of the Admiralty Sound region, James Ross Basin, Antarctica. *Cretaceous Res* 18:109–137
- Römer M, Torres M, Kasten S et al (2014) First evidence of widespread active methane seepage in the Southern Ocean, off the sub-Antarctic island of South Georgia. *Earth Planet Sci Lett* 403:166–177
- Ryan DR, Witts JD, Landman NH (2020) Palaeoecological analysis of a methane seep deposit from the Upper Cretaceous (Maastrichtian) of the U.S. Western Interior. *Lethaia* 54:185–203
- Schoepfer SD, Tobin TS, Witts JD, Newton RJ (2017) Intermittent euxinia in the high-latitude James Ross Basin during the latest Cretaceous and earliest Paleocene. *Palaeogeog Palaeoclim Palaeoecol* 477:40–54
- Speden IG (1970) The type Fox Hills Formation, Cretaceous (Maestrichtian), South Dakota. Systematics of the Bivalvia, *Bulletin of the Peabody Museum* 33. Yale University, p 222
- Stilwell JD, Zinsmeister WJ, Oleinik AE (2004) Early paleocene Mollusks of Antarctica: systematics, paleoecology and paleobiogeographic significance, 367th edn. Allen Press, Lawrence, p 89
- Tobin TS, Ward PD (2015) Carbon isotope ( $\delta^{13}\text{C}$ ) differences between Late Cretaceous ammonites and benthic mollusks from Antarctica. *Palaeogeog Palaeoclim Palaeoecol* 428:50–57
- Tobin TS, Ward PD, Steig EJ et al (2012) Extinction patterns,  $\delta^{18}\text{O}$  trends, and magnetostratigraphy from a southern high-latitude Cretaceous–Paleogene section: links with Deccan volcanism. *Palaeogeog Palaeoclim Palaeoecol* 350–352:180–188
- Tosolini A-MP, Cantrill DJ, Francis JE (2021) Paleocene high-latitude leaf flora of Antarctica Part 1: entire-margined angiosperms. *Rev Palaeobot Palynol* 285:104317
- Vaughan APM, Storey BC (2000) The eastern Palmer Land shear zone: a new terrane accretion model for the Mesozoic development of the Antarctic Peninsula. *J Geol Soc (London, U.K.)* 157:1243–1256
- Weller S (1903) The Stokes collection of Antarctic fossils. *J Geol* 11:413–419
- White CA (1890) On certain Mesozoic fossils from the Islands of St. Paul's and St. Peter's in the Straits of Magellan. *Proc US Nat Mus* 13:13–14
- Whittle RJ, Witts JD, Bowman VC et al (2019) Nature and timing of biotic recovery in Antarctic benthic marine ecosystems following the Cretaceous–Palaeogene mass extinction. *Palaeontology* 62:919–934
- Wilckens O (1910) Die Anneliden, Bivalven, und Gastropoden der Antarktischen Kreideformationen. *Wissenschaftliche Ergebnisse der Schwedischen Südpolar-Expedition, 1901–1903, vol 3, p 1–132*
- Witts JD, Bowman VC, Wignall PB et al (2015) Evolution and extinction of Maastrichtian (Late Cretaceous) cephalopods from the López de Bertodano Formation, Seymour Island, Antarctica. *Palaeogeog Palaeoclim Palaeoecol* 418:193–212
- Witts JD, Whittle RJ, Wignall PB et al (2016) Macrofossil evidence for a rapid and severe Cretaceous–Paleogene mass extinction in Antarctica. *Nat Commun* 7:11738
- Zinsmeister WJ (1988) Early geological exploration on Seymour Island, Antarctica. In: Feldmann RM, Woodburne MO (eds) *Geology and paleontology of Seymour Island, Antarctic Peninsula, Memoir 169. Geological Society of America, Boulder*, pp 1–16
- Zinsmeister WJ (1998) Discovery of fish mortality horizon at the K-T Boundary on Seymour Island: re-evaluation of events at the end of the Cretaceous. *J Paleontol* 72:556–571
- Zinsmeister WJ, Macellari CE (1988) Bivalvia (Mollusca) from Seymour Island, Antarctic Peninsula. In: Feldmann RM, Woodburne MO (eds) *Geology and paleontology of Seymour Island, Antarctic Peninsula, Memoir 169. Geological Society of America, Boulder*, pp 253–284